HIGH-PERFORMANCE CELLULOSE NANOFIBRIL COMPOSITE FILMS

Yan Qing,[a,b] Ronald Sabo,[b,*] Yiqiang Wu,[a] and Zhiyong Cai [b,*]

Cellulose nanofibril/phenol formaldehyde (CNF/PF) composite films with high work of fracture were prepared by filtering a mixture of 2,2,6,6-tetramethylpiperidine-1-oxyl (TEMPO) oxidized wood nanofibers and water-soluble phenol formaldehyde with resin contents ranging from 5 to 20 wt%, followed by hot pressing. The composites were characterized by tensile testing, dynamic mechanical analysis, scanning electron microscopy, atomic force microscopy, thermo-gravimetric analysis, and moisture/water absorption. Neat CNF films had tensile stress and Young's modulus of 232 MPa and 4.79 GPa, respectively. PF resin was found to be well dispersed in the composites, although the resin increased the roughness of the film surfaces. Hygroscopic capacities of the composites were dramatically reduced, as compared to neat films, in both high humidity environments and when soaked in water. The composites exhibited slightly reduced tensile strength with modestly increased storage modulus compared to neat CNF films. Remarkably, the work of fracture ranged from 20 to 27 MJ/m^3, making these films among the toughest reported for cellulose nanocomposites.

Keywords: Cellulose nanofibril; Phenol formaldehyde; Mechanical properties; Electron microscopy; Thermal degradation; Hygroscopic capacity

*Contact information: a: School of Materials Science and Engineering, Central South University of Forestry and Technology, 498 Shaoshan South Road, Changsha 410004, China; b: Forest Products Laboratory, United States Department of Agriculture, 1 Gifford Pinchot Drive, Madison 53726-2398, WI, USA; *Corresponding authors: rsabo@fs.fed.us(R Sabo); zcai@fs.fed.us (Z Cai)*

INTRODUCTION

Naturally occurring cellulose in wood, bamboo, help, flax, ramie, and other plants typically serves as the skeletal material or reinforcing component due to its excellent mechanical strength and special structure (Klemm *et al*. 2005; Siró and Plackett 2010). It has attracted growing interest to exploit this reinforcing potential in composite materials.

Cellulose nanofibrils (CNFs) isolated from bleached pulp fiber suspension by vigorous mechanical shear and impact were first introduced by Herrick and Turbak in 1983 (Herrick *et al.* 1983; Turbak *et al.* 1983). The elastic modulus of similar cellulose nanofibers has been experimentally measured to be about 150 GPa (Iwamoto *et al.* 2009), and films created from CNFs have been reported to have excellent mechanical properties (Hubbe *et al.* 2008; Siró and Plackett 2010). An orientated TEMPO oxidized CNF film achieved an unexpectedly high elastic modulus of 33 GPa and a tensile strength of 400 MPa (Sehaqui *et al.* 2012). In addition to outstanding mechanical performance and the unique web-like network structure, CNFs exhibit other advantages including their abundance, light weight, high aspect ratio, and accessible reactivity due to the presence of

a high surface area of hydroxyl groups (Zimmermann *et al.* 2010). Therefore, in the past decade there has been increasing interest in utilizing CNFs in polymer reinforcement not only in hydrophilic matrices such as starch, polyvinyl alcohol (PVA), amylopectin, chitosan, and aqueous urea formaldehyde, but also in hydrophobic substrates like polylactic acid (PLA) and polypropylene (PP) (Dufresne and Vignon 1998; Lu *et al.* 2008; Plackett *et al.* 2010; Fernandes *et al.* 2010; Veigel *et al.* 2011; Iwatake *et al.* 2008; Cheng *et al.* 2007). Despite enormous potential application, challenges remain to disperse hydrophilic nanofibers into nonpolar polymers and to improve interfacial bonding strength between the two different phases (Hubbe *et al.* 2008; Siró and Plackett 2010).

Conventional water-soluble thermosetting resins have previously been impregnated into CNF sheets. Nakagaito and Yano (2005) developed nanocomposites with high bending strength (370 MPa) and Young's modulus (16 GPa) by stacking and pressing 25 layers of thin phenol formaldehyde (PF) resin immersed CNF mats at 160 °C for 30 min at 100 MPa. Notably, such strength is about twice that of pulp-based composites under the same condition and is comparable to magnesium alloy. Similarly, Henriksson and Berglund (2007) prepared 70 μm-thick CNF nanocomposites containing melamine formaldehyde (MF); the tensile strength and Young's modulus were improved by 50% and 30%, respectively, at 5% MF content. These nanocomposites were brittle but semitransparent and stiff, which is related to the natural characteristics of MF resin. Nakagaito and Yano (2008) also tested the mechanical and thermal expansion properties of CNF biocomposites with high PF resin contents from 20% to 80% and they found that Young's modulus decreased, while the coefficient of thermal expansion increased, with increasing PF dosage. In addition, highly flexible, ductile, and optically transparent nanocomposites with very low thermal expansion were obtained by impregnating low Young's modulus acrylic resin into CNF sheets (Iwamoto *et al.* 2005; Okahisa *et al.* 2009). However, no report in the literature was found in which CNF slurry and water-soluble PF resin were first mixed prior to forming into a composite film.

In the present work, the objective was to prepare flexible, minimally hygroscopic CNF films that can be used for a variety of applications, such as substrates for fast electronics. Here, a novel method for preparing CNF/PF composites by firstly mixing an aqueous slurry of the components prior to ultrafiltration and hot compression is presented. The effects of PF contents on tensile performance, dynamic-mechanical properties, thermal degradation behavior, and hygroscopic capacity were examined.

EXPERIMENTAL PROCEDURE

Materials

TEMPO-oxidized cellulose nanofibrils used in this experiment were prepared according to the work reported by Saito *et al.* (2009), as briefly described here. Commercially-supplied fully bleached eucalyptus pulp was carboxylated using 2,2,6,6-tetramethylpiperidinyl-1-oxyl (TEMPO), sodium chlorite, and sodium hypochlorite as the reactants at 60 °C for 48 hours. TEMPO-oxidized pulp fibers then were washed thoroughly using distilled water and homogenized in a disperger to break apart fiber bundles. The fiber slurry was diluted to facilitate separation of coarse and fine fractions

by centrifuging at 12000 g, and the coarse fraction was rejected. The nanofiber suspension was concentrated to a solid content of approximately 0.4% using ultrafiltration. A final clarification step was performed, in which the nanofiber dispersion was passed once through an M-110EH-30 Microfluidizer (Microfluidics, Newton, MA) with 200- and 87-μm chambers in series.

The PF resin (GP®169C21 RESI-BOND®) used was a commercially available product normally used for fiberboard preparation and had a solid content of 50.5%.

Fabrication of CNF Film and CNF/PF Nanocomposites

To prepare CNF films, 0.4 wt% CNF slurries were first diluted in distilled water and vigorously stirred for 30 min to obtain a well dispersed nanofiber suspension. When preparing CNF/PF nanocomposites, PF resin was added into CNF suspension and mixed with distilled water to produce composites with final resin concentrations of 5%, 10%, 15%, and 20%. The suspensions were then filtered under approximately 0.55 MPa of air pressure in a Hazardous Waste Filtration System (Millipore Cat. No. YT30 142HW, Millipore Corporation, USA). The nanomembrane (Omnipore membrane model JVWP14225, Millipore corporation, USA) used in the apparatus had a pore size of 0.1 μm and was supported by Whatman P2 filter paper (Fisher Scientific, USA).

Wet CNF and CNF/PF films were separated from the nanomembrane and individually placed between waxy coated paper and filter papers to absorb excess water. The films and absorbing paper were then placed between two metal plates to avoid out-of-plane deformation. When solid content increased to about 30%, a 23 kg weight was placed on the assembly. Throughout the drying process, several changes of the absorbing papers were made to facilitate the drying of a relatively wrinkle-free film. The sandwiched films with approximately 80 to 90% solids content were put in an oven at 60 °C for 8 h, followed by conditioning in a humidity room at 65% relative humidity (RH) and 27 °C for more than 24 h. Finally, the conditioned films were hot pressed at 130 °C and 30 MPa for 1 min between two special steel cauls with reported surface roughness of 0.2 nm to produce a smooth surface. The films and composites thus obtained had diameters of 120 mm and thicknesses from 0.09 mm to 0.12 mm.

Tensile Performance

Tensile properties of CNF films and CNF/PF nanocomposites were tested according to ASTM D638-10 (2010), although extension was taken to be the cross-head displacement, and the gage length was taken to be the narrow section of the dog-bone specimens. The specimens were cut to conform to ASTM D638-10 type V dogbone shape using a die (Qualitest, Ft. Lauderdale, FL, USA). All samples were conditioned at 50% RH and 27 °C for 1 week before the testing. The test was carried out in a room conditioned at 50% RH and 23 °C using an Instron 5865 universal materials testing machine with a 500 N load cell. The cross-head speed was 1 mm/min, and the specimens were pre-loaded at 10 N to remove slack. At least 5 specimens were tested for each condition. The work of fracture was calculated by numerical integration of the stress-strain curve. Modulus of elasticity was calculated as the slope of the stress-strain curve in the stress region of 30 to 70 MPa. Film densities were calculated gravimetrically by

measuring the dimensions and weight of multiple well-defined sections of each film, and more than 5 specimens were measured for each material.

Dynamic Mechanical Properties

The dynamic mechanical analysis was performed in tension mode with film/fiber clamps with a Q800 DMTA (TA-Instrument, New Castle, DE, USA). Rectangular specimens (30 mm length × 6 mm width) had thicknesses ranging from 0.09 mm to 0.12 mm. Measurements were conducted at a heating rate of 5 °C/min from -50 °C to 200 °C with an amplitude of 5 μm at a frequency of 1 Hz. Dried specimens were cooled to -50 °C with liquid nitrogen and held at that temperature for 10 min.

Thermal Degradation

Thermogravimetric analysis (TGA) of samples was performed using a Perkin Elmer TGA-7 (Perkin Elmer, Waltham, MA, USA). Before testing, specimens were oven-dried at a temperature of 105 °C for 6 h to evaporate the residual water, and about 7 to 10 mg of the powder was placed into the instrument. The weight was recorded from 50 °C to 600 °C as the temperature was ramped at a heating rate of 10 °C /min with a 10 min hold at 105 °C. A high purity nitrogen stream at the flow rate of 20 mL/min was continuously passed into the furnace when testing.

Scanning Electron Microscopy

The surface of cut cross and fracture section for CNF films and composites were examined using a Zeiss EVO40 scanning electron microscope (Carl Zeiss SMT, INC., Thornwood, NY, USA). The cross-section of the films was obtained by cutting with a steel blade, and fracture surfaces were obtained by breaking notched specimens. The specimens were affixed to a carbon tape substrate and coated with a thin layer of gold-palladium alloy.

Atomic Force Microscopy

Atomic Force Microscopy (AFM) scans were performed on the surface of the films using a Quesant (Agoura Hills, CA, USA) atomic force microscope in tapping mode. The scan size was 40 μm × 40 μm at a scan rate of 4 Hz and a resolution of 600 lines × 600 points. Small rectangular samples (approximately 3 mm × 3 mm) were affixed to AFM stubs using a two-part epoxy. Four locations on each specimen were scanned and averaged for surface roughness calculations.

Moisture and Water Absorption

Hygroscopic characteristic of CNF films and CNF/PF nanocomposites were evaluated by equilibrating samples at various levels of relative humidity and by soaking specimens in distilled water. For moisture absorption-desorption tests, rectangular specimens (10 mm × 6 mm) were stored at 27 °C and 30% RH, 65% RH, and 90% RH for at least 4 days for each condition until equilibrium was reached. After evaluating weight changes of the samples at increasing levels of humidity, samples were then placed back into the conditioning rooms in decreasing order of humidity to evaluate both absorption and desorption of moisture. Thereafter, specimens were oven dried at a

temperature of 105 °C. To measure water absorption capacity, rectangular specimens with the same dimension as the moisture absorption-desorption test were first conditioned at 50% RH and 27 °C for a week, and soaked in distilled water at a temperature of 20 °C. Samples were blotted with filter paper and weighed every half hour until stable. At least 5 specimens were tested for each sample.

RESULTS AND DISCUSSION

Physical and Mechanical Properties

CNF films are dense and formed by collapse of web-like nanoscale fiber networks in lamellar structures. Direct immersion of dry CNF films, even with a porosity of about 15%, in aqueous PF resin solutions was found by the authors to be insufficient to impregnate the films with substantial amounts of resin. Researchers have found other successful methods for impregnating resins into these films. For example, water-soluble phenol formaldehyde and melamine formaldehyde were impregnated into porous CNF film by different methods, such as vacuum (Nakagaito and Yano 2005) and methanol immersion. Alternatively, we present here a novel method of forming CNF/PF composites by first mixing the nanofibers in resin, followed by ultrafiltration and hot-pressing. The resulting films were translucent, flexible, smooth, and exceptionally tough.

Representative stress-strain curves for the neat and composite films are shown in Fig. 1, and the various tensile properties are detailed in Table 1. CNF and CNF/PF films possess excellent mechanical properties. The work of fracture values measured here are greater than any other reported values known to the authors. For example, the presently obtained values for neat films (20.5 MJ/m^3) are about 30% higher than those reported by Henriksson *et al.* (2008) and more than 4-fold higher than for films prepared by Henriksson and Berglund (2007), which were hot-pressed at 160 °C for 10 min at a pressure of 30 MPa. The high work of fracture for films prepared in this study manifests itself largely in the form of larger-than-usual strains at break. Here, strains at break averaged between about 13 % and 17 %, whereas others have typically reported strains below ten percent at break.

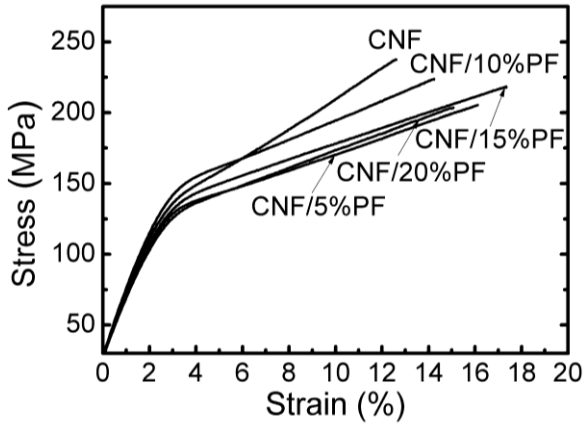

Fig. 1. Typical stress-strain curves for CNF and CNF/PF composite films

A number of factors may have led to the extremely high work of fracture values reported here. For instance, the neutral pH, TEMPO-mediated oxidation scheme for preparing cellulose nanofibers appears to result in CNF films that are much tougher than films prepared from other methods (Siró and Plackett 2010; Saito *et al.* 2009). The degrees of polymerization of nanofibers created under this condition are reportedly high (up to about 1000), and films made from high-DP nanofibers were previously shown to have greater strength and toughness than those with lower DP (Saito *et al.* 2009; Heriksson *et al.* 2008). The density of the films in this study are quite high (1450 kg/m^3) compared to other studies, and the density of composites is known to be a good indicator of composite strength (Takagi and Asano 2008). The preparation method also seems to be an important factor affecting mechanical properties. Here, the ultrafiltration and drying processes were particularly slow, and after mild drying of the sheets at 60 °C, they were allowed to absorb moisture at elevated humidity prior to pressing. Such processing may have allowed for residual stresses to be removed from the films. Furthermore, variations in test procedures throughout the literature might account for some of the differences in measured mechanical properties. For example, Henriksson *et al.* (2008) used rectangular specimens 40 mm in length at a tensile test speed of 4 mm/min (10 %/min), whereas the test region of the dogbone samples in the current study was about 8 mm at a test speed of 1 mm/min (12 %/min). They also employed a more rigorous method of measuring strain via a video extensometer. In other reports, no mention of the method of evaluation strain was made, so some caution is warranted in making direct comparison of various results presented here and elsewhere in the literature. Further studies are necessary to understand the full impact of processing conditions, fiber source, and fibrillation procedures on mechanical properties.

Table 1. Physical and Mechanical Properties of CNF and CNF/PF Films

Sample	Thickness (μm)	Density (kg/m^3)	Strain at break (%)	Stress at break (MPa)	Young's modulus (GPa)	Work of fracture (MJ/m^3)
CNF	94±1.4	1483±16	12.6±1.9	232±22	4.79±0.14	20.5±4.4
CNF/5%PF	108±2.9	1455±24	14.5±2.5	201±10	4.53±0.16	22.1±4.6
CNF/10%PF	111±1.1	1467±16	12.6±1.9	214±14	4.84±0.12	20.3±4.2
CNF/15%PF	118±2.4	1454±14	16.8±2.3	216±11	4.38±0.08	27.3±4.8
CNF/20%PF	122±1.3	1435±10	14.7±2.3	201±15	4.16±0.16	21.9±4.5

From the test data, the introduction of PF generally had little effect on the tensile properties of the composites, and an analysis of variance (ANOVA) reveals only a few significant differences among the various tensile properties of the composites prepared. The neat films appear to be statistically (at $\alpha = 0.05$) stronger than the composites with 5% and 20% PF resin but not those with 10% and 15% resin content. The modulus of the composite with 20% resin was also shown to be statistically smaller than the other films. While the small differences and small sample size warrant caution in making concrete conclusions regarding the relative tensile properties of the various composites, similar results were found by Nakagaito and Yano (2005), in which the bending strength and stiffness of CNF/PF laminated composites peaked in the 10 to 15% PF resin range. Interestingly, the strain at break of the composites was apparently greater than for neat films. The ductility of the composites is somewhat surprising, since PF resin is notably

brittle. Perhaps the resin acted to bridge the layers of the CNF lamellar structure, preventing crack propagation. Nonetheless, both the CNF/PF composites and CNF neat films in this study had good tensile strength, modest stiffness, and exceptional toughness.

Morphology Characterization

SEM images of the CNF and CNF/PF films were taken to examine the microstructure of the materials, and Fig. 2 shows the cut cross-sections (top) and fractured cross-sections (bottom) of neat (left) and composite (right) films. The lamellar structure of the nanocellulose is clear in the cross-section of the neat films as well as the composites. The PF resin appears well-dispersed between the nanofibers and the layers. In combination with density data, the SEM micrographs show that dense, layered, paper-like films and nanocomposites were obtained.

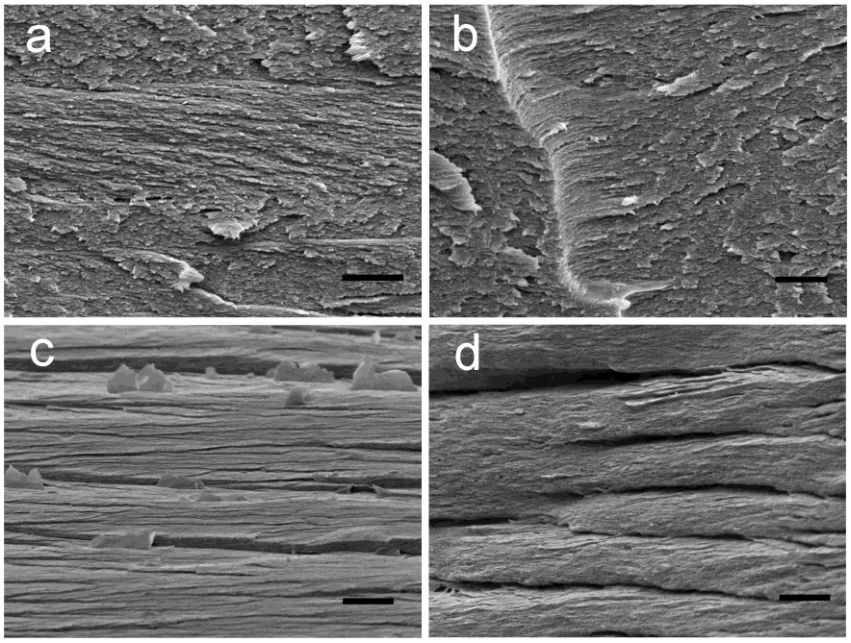

Fig. 2. SEM images of cross surface (a and b) and fracture surface (c and d) for CNF (a and c) and CNF/15%PF composite films (b and d). The scale bars are 5 μm.

Atomic force microscopy images of the surface of the films are shown in Fig. 3. The film surfaces are smooth, and the resin appears well distributed on the surface and throughout the cross-section. As the resin concentration is increased, the size of the resin domains appears to increase. An analysis of the topology of the film surfaces reveals that the roughness increases with increasing resin concentration. The roughness of the neat CNF films and those with 5% and 15% PF resin were measured to be 54.2 ± 15 nm, 127 ± 25 nm, and 234 ± 61 nm, respectively. These roughness values are much higher than the roughness of the mirror-polished plates between which the films were hot pressed. Andresen *et al.* (2006) found similar results with silylated CNFs and suggest that the more hydrophobic materials are squeezed out as the cellulose hydrogen bonds upon drying, resulting in rougher composites than neat films. The PF resin also may cure in domains that are unable to flow during hot pressing. Maintaining a smooth surface is

desirable for many applications, including those in which electronics are assembled on the surface. While, the minimum surface roughness is not yet completely understood, the procedure described herein for making films results in dramatically reduced surface roughness compared to procedures in which filter or blotter papers are used to absorb the water during pressing.

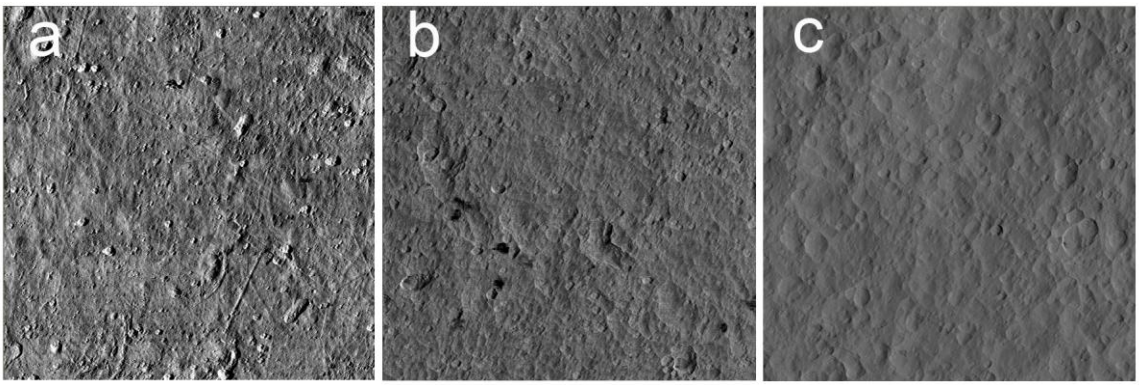

Fig. 3. AFM phase images of the surface of neat CNF (a) and CNF/PF composite films with 5% (b) and 15% (c) PF resin. The scan area for these images is 40 μm × 40 μm.

Dynamic Mechanical Properties

Figure 4 shows the storage modulus for CNF film and CNF/PF composites as a function of temperature. The maximum storage modulus for the films ranged from 14 GPa to 16 GPa at a temperature of -50 °C, and it was reduced gradually to about 6.5 GPa as the temperature increased to 200 °C. The high storage modulus is explained by the formation of nanofibril networks as water is removed during drying of the films (Svagan *et al*. 2007). The addition of PF slightly increased the storage modulus by up to 2 GPa. While this indicates that the stiffness of the composite was higher compared to neat CNF films, the same result was not observed for static tensile stiffness.

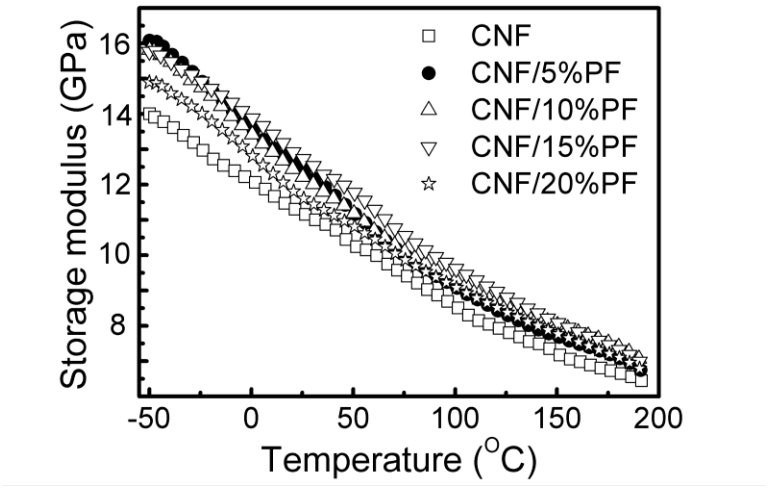

Fig. 4. Storage modulus as a function of temperature for CNF and CNF/PF composite films

Thermogravimetric Analysis

The thermal stability and degradation of CNFs, PF, and composites with 10 wt% PF was examined by TGA, and results are presented in Fig. 5. Since nanocellulose is highly hygroscopic, the weight loss is presented based on the sample weight after the samples were held at 105 °C. The cured PF resin degraded gradually, and there was approximately 67% char yield at a temperature of 600 °C. The major thermal degradation peak of PF resin appeared at 253 °C, which can be seen in the DTG curve (Fig. 5b). The most pronounced thermal degradation peaks for both CNF and CNF/PF composites happened at 285 °C and 345 °C. Similarly, Alemdar and Sain (2008) reported that nanocellulose from agricultural residues started to thermally degrade above 290 °C, which is nearly 100 °C higher than for the natural original fibers. The enhancement in thermal stability facilitates the use of these nanofibers for use in polymer composites.

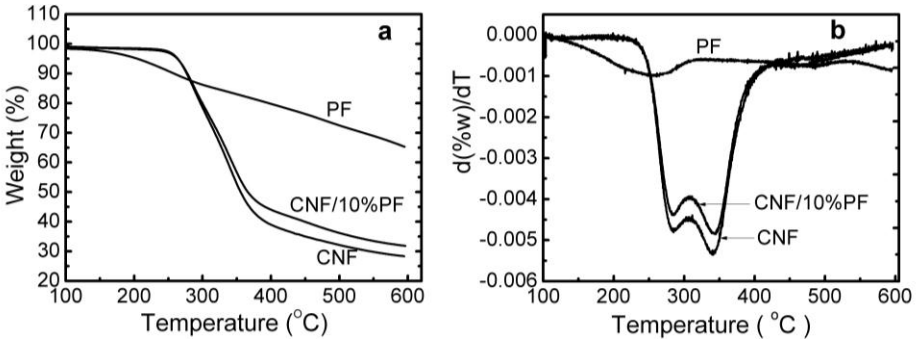

Fig. 5. TG (a) and DTG (b) for PF, CNF and CNF/10%PF composite

Moisture and Water Absorption Characteristic

The hygroscopic characteristic of CNF films and composites were examined by testing specimens in various moisture contents and by soaking them in distilled water. The absorption and desorption of moisture by the films is shown in Fig. 6. At relative humidity levels at or below 65%, neat films and composites had roughly the same moisture content. However, neat CNF films had higher absorbed moisture than the composites at 90% RH.

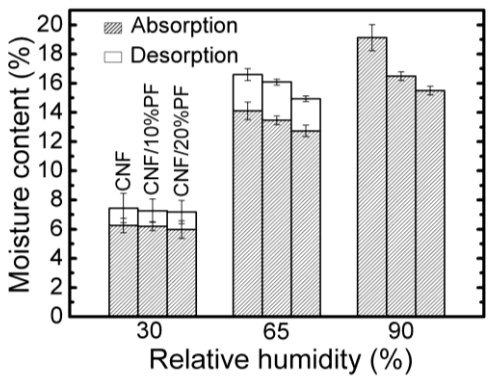

Fig. 6. Absorption and desorption for CNF and CNF/PF composite films (10% and 20% content)

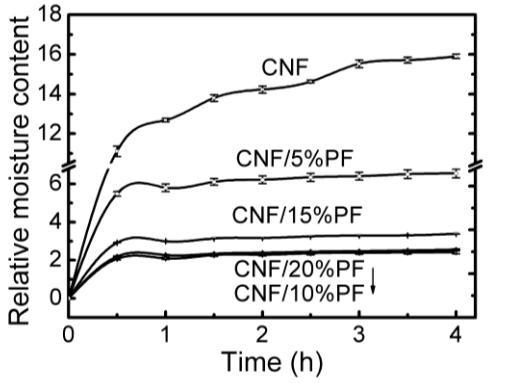

Fig. 7. Water absorption for CNF and CNF/PF composite films soaked in distilled water

The difference in water absorption capacities between neat films and composites was obvious when CNF films and composites were soaked in water. The relative weights of the films soaked in water are shown in Fig. 7 (relative moisture content = [current weight-original weight]/original weight). The neat CNF films gained 16 times its original weight after soaking for four hours, whereas the weight of CNF/PF films with 10 to 20% PF gained 2 to 3 times their weight in water. The composite with 15% PF resin gained slightly more weight than the composites with 10 or 20% PF resin, which may be an anomaly. The weight gain of the composites was mostly maximized after about 0.5 h, whereas the neat film continued to gain weight at 4 h.

Christensen summarized the swelling mechanism of wood cell wall in water and alcohol as involving two stages: 1) wetting and adsorption at capillary surfaces and 2) molecular penetration and swelling (Christensen 1967). When CNF films are subjected to high moisture environments, the hydrogen bonds between nanofibers are dissociated and replaced by hydrogen bonds between nanofibers and water (Aulin *et al.* 2010). The dense structure is broken, and more water is absorbed into NFC films. In case of composites with PF resin, ether linkages react between methylol groups of phenolic resin and hydroxyl groups are formed and remain stable in water (Nakagaito and Yano 2008), thus the thickness swelling is stabilized and hydrogen bonds substitution is limited.

CONCLUSIONS

Flexible CNF and cellulose nanocomposite films were successfully prepared by ultrafiltration of CNF suspensions and CNF/PF mixtures, respectively, followed by dewatering and hot-pressing. The films were found to be translucent, dense, and layered, with exceptional toughness. The best tensile properties shown for the CNF films here resulted in a stress at break of 232 MPa and Young's modulus of 4.8 GPa. Both CNF and composites had work of fracture values of more than 20 MJ/m^3. The introduction of PF resin into the composite had only little effect of the mechanical properties of the films but resulted in greatly reduced water absorption. Based on the results obtained, 10 to 15% resin is arguably the optimal concentration for CNF/PF composites, since further addition did not improve water resistance and appears to impair mechanical properties. Further investigation into the vapor transmission and thermal expansion are warranted, as CNF nanocomposites with PF resin have promising potential in applications including packaging and barrier materials and as substrates for fast flexible electronics.

ACKNOWLEDGEMENTS

Enormous gratitude is offered to Rick Reiner for preparing and supplying cellulose nanofibers. The authors would also like to acknowledge Benjamin Treml for help with tensile testing. Tom Kuster and Jane O'Dell are kindly acknowledged for SEM and DMTA tests, respectively. The authors would also like to thank Joseph Jakes and Jane O'Dell for performing AFM scans. This work was partly supported by the national "948" project of China (2009-4-51).

REFERENCES CITED

Alemdar, A., and Sain, M. (2008). "Isolation and characterization of nanofibers from agricultural residues-Wheat straw and soy hulls," *Bioresour. Technol.* 99(6), 1664-1671.

Andresen, M., Johansson, L.-S., Tanem, B. S., and Stenius, P. (2006). "Properties and characterization of hydrophobized microfibrillated cellulose," *Cellulose* 13(6), 665-677.

ASTM. (2010). *Annual Book of ASTM Standards*, ASTM D638-10: "Standard test method for tensile properties of plastics," ASTM International, West Conshohockon, PA.

Aulin, C., Gällstedt, M., and Lindström, T. (2010). "Oxygen and oil barrier properties of microfibrillated cellulose films and coatings," *Cellulose* 17(3), 559-574.

Cheng, Q., Wang, S., Rials, T. G., and Lee, S. H. (2007). "Physical and mechanical properties of polyvinyl alcohol and polypropylene composite materials reinforced with fibril aggregates isolated from regenerated cellulose fibers," *Cellulose* 14(6), 593-602.

Christensen, G. N. (1967). "Sorption and swelling within wood cell walls," *Nature* 213(5078), 782-784.

Dufresne, A., and Vignon, M. R. (1998). "Improvement of starch film performances using cellulose microfibrils," *Macromolecules* 31(8), 2693-2696.

Fernandes, S. C. M., Freire, C. S. R., Silverstre, A. J. D., Neto, C. P., Gandini, A., Berglund, L. A., and Salmén, L. (2010). "Transparent chitosan films reinforced with a high content of nanofibrillated cellulose," *Carbohydr. Polym.* 81(2), 394-401.

Henriksson, M., and Berglund, L. A. (2007). "Structure and properties of cellulose nanocomposite films containing melamine formaldehyde," *J. Appl. Polym. Sci.* 106(4), 2817-2824.

Heriksson, M., Berglund, L. A., Isaksson, P., Lindström, T., and Nishino, T. (2008). "Cellulose nanopaper structure of high toughness," *Biomacromolecules* 9(6), 1579-1585.

Herrick, F. W., Casebier, R. L., Hamilton, J. K., and Sandberg, K. R. (1983). "Microfibrillated cellulose: Morphology and accessibility," *J. Appl. Polym. Sci. Appl. Polym. Symp.* 37(9), 797-813.

Hubbe, M. A., Rojas, O. J., Lucia, L. A., and Sain M. (2008). "Cellulosic nanocomposites: A review," *BioResources* 3(3), 929-980.

Iwamoto, S., Nakagaito, A. N., Yano, H., and Nogi, M. (2005). "Optically transparent composites reinforced with plant fiber-based nanofibers," *Appl. Phys. A.* 81(6), 1109-1112.

Iwamoto, S., Kai, W., Isogai, A., and Iwata, T. (2009). "Elastic modulus of single cellulose microfibrils from tunicate measured by atomic force microscopy," *Biomacromolecules* 10(9), 2571-2576.

Iwatake, A., Nogi, M., and Yano, H. (2008). "Cellulose nanofiber-reinforced polylactic acid," *Compos. Sci. Technol.* 68(9), 2103-2106.

Klemm, D., Heublein, B., Fink, H. -P., and Bohn, A. (2005). "Cellulose: Fascinating biopolymer and sustainable raw material," *Angew. Chem. Int. Ed.* 44(22), 3358-3393.

Lu, J., Wang, T., and Drzal, L. T. (2008). "Preparation and properties of microfibrillated cellulose polyvinyl alcohol composite materials," *Compos. A* 39(5), 738-746.

Nakagaito, A. N., and Yano, H. (2005). "Novel high-strength biocomposites based on micro fibrillated cellulose having nano-order-unit web-like network structure," *Appl. Phys. A* 80(1), 155-159.

Nakagaito, A. N., and Yano, H. (2008). "The effect of fiber content on the mechanical and thermal expansion properties of biocomposites based on microfibrillated cellulose," *Cellulose* 15(4), 555-559.

Okahisa, Y., Yoshida, A., Miyaguchi, S., and Yano, H. (2009). "Optically transparent wood-cellulose nanocomposites as a base substrate for flexible organic light-emitting diode displays," *Compos. Sci. Technol.* 69(11-12), 1958-1961.

Plackett, D., Anturi, H., Hedenqvist, M., Ankerfors, M., Gällstedt, M., Lindström, T., and Siró, I. (2010). "Physical properties and morphology of films prepared from microfibrillated cellulose and microfibrillated cellulose in combination with amylopectin," *J. Appl. Polym. Sci.* 117(6), 3601-3609.

Saito, T., Hirota, M., Tamura, N., Kimura, S., Fukuzumi, H., Heux, L., and Isogai, A. (2009). "Individualization of nano-sized plant cellulose fibrils by direct surface carboxylation using TEMPO catalyst under neutral conditions," *Biomacromecules* 10(7), 1992-1996.

Sehaqui, H., Mushi, N. E., Morimune, S., Salajkova, M., Nishino, T., and Berglund, L. A. (2012). "Cellulose nanofiber orientation in nanopaper and nanocomposites by cold drawing," *Appl. Mater. Interfaces* 4(2), 1043-1049.

Siró, I., and Plackett, D. (2010). "Microfibrillated cellulose and new nanocomposites materials: A review," *Cellulose* 17(3), 459-494.

Svagan, A. J., Azizi Samir, M. A. S., and Berglund, L. A. (2007). "Biomimetic polysaccharide nanocomposites of high cellulose content and high toughness," *Biomacromolecules* 8(8), 2556-2563.

Takagi, H., and Asano, A. (2008). "Effects of processing conditions on flexural properties of cellulose nanofiber reinforced "green" composites," *Compos. A* 39(4), 685-689.

Turbak, A. F., Snyder, F. W., and Sandberg, K. R. (1983). "Microfibrillated cellulose, a new cellulose product: Properties, uses, and commercial potential," *J. Appl. Polym. Sci. Appl. Polym. Symp.* 37(9), 815-827.

Veigel, S., Müller, U., Keckes, J., Obersriebnig, M., and Gindl-Altmutter, W. (2011). "Cellulose nanofibrils as filler for adhesive: effect on the specific fracture energy of solid wood-adhesive bonds," *Cellulose* 18(5), 1227-1237.

Zimmermann, T., Bordeanu, N., and Sturb, E. (2010). "Properties of nanofibrillated cellulose from different raw materials and its reinforcement potential," *Carbohydr. Polym.* 79(4), 1086-1093.

Article submitted: March 12, 2012; Peer review completed: May 19, 2012; Revised version received and accepted: May 25, 2012; Published: May 29, 2012.